J|A|C|S
ARTICLES
Published on Web 03/03/2007

Antibody-Catalyzed Oxidation of Δ^9-Tetrahydrocannabinol

Andrew P. Brogan,[†] Lisa M. Eubanks,[†] George F. Koob,[‡] Tobin J. Dickerson,*[,†] and Kim D. Janda*[,†]

Contribution from the Departments of Chemistry and Immunology, The Skaggs Institute for Chemical Biology, Worm Institute for Research and Medicine, and the Committee on the Neurobiology of Addictive Disorders, The Scripps Research Institute, 10550 North Torrey Pines Road, La Jolla, California 92037

Received January 2, 2007; E-mail: kdjanda@scripps.edu; tobin@scripps.edu

Abstract: Marijuana abuse continues to plague society and the lack of effective treatments warrants concern. Catalytic antibodies capable of oxidatively degrading the major psychoactive component of marijuana, Δ^9-tetrahydrocannabinol (Δ^9-THC), are presented. The antibodies generate reactive oxygen species from singlet oxygen ($^1O_2$*), using riboflavin (vitamin B_2) and visible light as the $^1O_2$* source. Cannabitriol was identified as the major degradation product of this reaction, demonstrating the ability of an antibody to catalyze a complex chemical transformation with therapeutic implications for treating marijuana abuse.

Introduction

Δ^9-Tetrahydrocannabinol (Δ^9-THC) is the active component of marijuana and the most commonly abused illicit drug in the U.S.[1,2] Marijuana use often leads to abuse of other illicit drugs as postulated by the "cannabis gateway hypothesis"[3] and supported by clinical evidence and numerous population surveys.[4−6] Furthermore, exposure to Δ^9-THC increases opiate self-administration in an animal model by specifically altering the endogenous opioid system, providing a molecular basis for the gateway hypothesis.[7] Currently, there are no clinical treatments for marijuana abuse. A promising approach to combat drug abuse is immunopharmacotherapy, where active or passive immunizations are administered to bind the target drug before it can reach its cognate receptor. Using this strategy, approaches to treat cocaine, nicotine, PCP, and methamphetamine abuse have been reported.[8] However, this method is limited by the need for stoichiometric amounts of antibody to bind the target drug; in contrast, a catalytic antibody capable of decomposing the drug presents a more advantageous substoichiometric system.

A wide range of chemical transformations have been accelerated by catalytic antibodies, primarily using transition state analogues or reactive immunization.[9] Several cocaine esterase antibodies have been generated by replacing the cocaine benzyl ester with a phosphonate ester as a mimic of the hydrolysis transition state.[10−12] Unfortunately, no obvious route for an antibody-catalyzed reaction is apparent when examining the structure of Δ^9-THC; although, the C9−C10 olefin is expected to be susceptible to oxidation. Oxidation reactions have proven difficult to program into the antibody combining site; however, a new paradigm in antibody catalysis was recently reported by Lerner and co-workers, where all antibodies were found to have the intrinsic ability to destroy their corresponding antigen by generating reactive oxygen species (ROS) from singlet oxygen ($^1O_2$*).[13−17] Examples of potential ROS generated by antibodies include hydrogen peroxide (H_2O_2), ozone (O_3), and superoxide (O_2^-), enabling a range of different reactions. We recently reported a potential therapeutic application of this phenomenon by demonstrating the antibody-catalyzed oxidative degradation of nicotine into putatively pharmacologically inactive products using visible light and riboflavin (vitamin B_2), a known photosensitizer, as the singlet oxygen source.[18] On the basis of

[†] Departments of Chemistry and Immunology, The Skaggs Institute for Chemical Biology, and the Worm Institute for Research and Medicine.
[‡] Committee on the Neurobiology of Addictive Disorders.

(1) *Substance Abuse and Mental Health Services Administration. Results from the 2001 National Household Survey on Drug Abuse. Summary of National Findings*; NHSDA Series H-17, DHHS Publication SMA 02−3758; Office of Applied Studies, U.S. Department of Health and Human Services: Rockville, MD, 2002; Vol. I.
(2) Johnston, L. D.; O'Malley, P. M.; Bachman, J. G. *Monitoring the Future National Survey Results on Drug Use, 1975−2002*; National Institute on Drug Abuse: Bethesda, MD, 2003.
(3) Kandel, D. *Science* **1975**, *190*, 912−914.
(4) Kandel, D. *Stages and Pathways of Drug Involvement: Examining the Gateway Hypothesis;* Cambridge University Press: Cambridge, U.K., 2002.
(5) Fergusson, D. M.; Boden, J. M.; Horwood, L. J. *Addiction* **2006**, *101*, 556−569.
(6) Kandel, D. B. *JAMA, J. Am. Med. Assoc.* **2003**, *289*, 482−483.
(7) Ellgren, M.; Spano, S. M.; Hurd, Y. L. *Neuropsychopharmacology* **2007**, *32*, 607−615.
(8) Meijler, M. M.; Matsushita, M.; Wirsching, P.; Janda, K. D. *Curr. Drug Discov. Technol.* **2004**, *1*, 77−89.
(9) Xu, Y.; Yamamoto, N.; Janda, K. D. *Bioorg. Med. Chem.* **2004**, *12*, 5247−5268.
(10) Landry, D. W.; Zhao, K.; Yang, G. X.; Glickman, M.; Georgiadis, T. M. *Science* **1993**, *259*, 1899−1901.
(11) Yang, G.; Chun, J.; Arakawa-Uramoto, H.; Wang, X.; Gawinowicz, M. A.; Zhao, K.; Landry, D. W. *J. Am. Chem. Soc.* **1996**, *118*, 5881−5890.
(12) Matsushita, M.; Hoffman, T. Z.; Ashley, J. A.; Zhou, B.; Wirsching, P.; Janda, K. D. *Bioorg. Med. Chem. Lett.* **2001**, *11*, 87−90.
(13) Wentworth, A. D.; Jones, L. H.; Wentworth, P., Jr.; Janda, K. D.; Lerner, R. A. *Proc. Natl. Acad. Sci. U.S.A.* **2000**, *97*, 10930−10935.
(14) Wentworth, P., Jr.; Jones, L. H.; Wentworth, A. D.; Zhu, X.; Larsen, N. A.; Wilson, I. A.; Xu, X.; Goddard, W. A., III; Janda, K. D.; Eschenmoser, A.; Lerner, R. A. *Science* **2001**, *293*, 1806−1811.
(15) Wentworth, P., Jr.; Nieva, J.; Takeuchi, C.; Galve, R.; Wentworth, A. D.; Dilley, R. B.; DeLaria, G. A.; Saven, A.; Babior, B. M.; Janda, K. D.; Eschenmoser, A.; Lerner, R. A. *Science* **2003**, *302*, 1053−1056.
(16) Wentworth, P., Jr.; Wentworth, A. D.; Zhu, X.; Wilson, I. A.; Janda, K. D.; Eschenmoser, A.; Lerner, R. A. *Proc. Natl. Acad. Sci. U.S.A.* **2003**, *100*, 1490−1493.
(17) Zhu, X.; Wentworth, P., Jr.; Wentworth, A. D.; Eschenmoser, A.; Lerner, R. A.; Wilson, I. A. *Proc. Natl. Acad. Sci. U.S.A.* **2004**, *101*, 2247−2252.

 10.1021/ja070022m CCC: $37.00

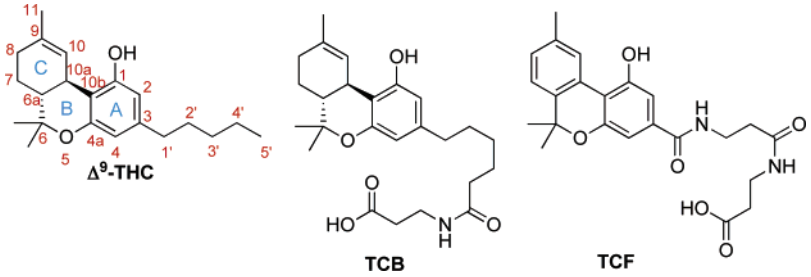

Figure 1. Structures of Δ⁹-tetrahydrocannabinol (Δ⁹-THC) and TCB and TCF haptens.

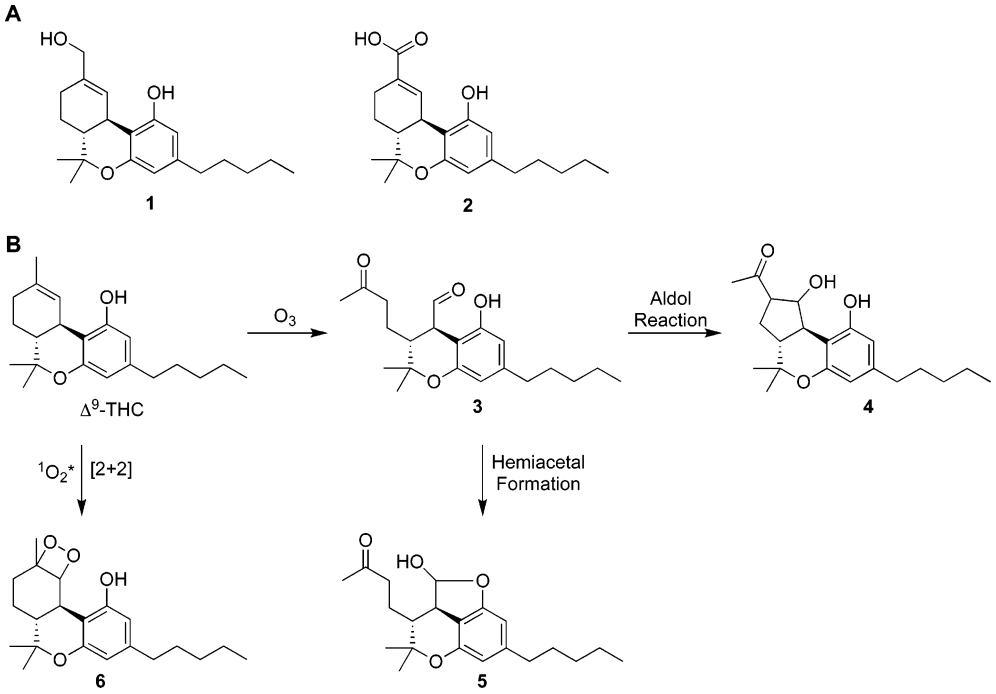

Figure 2. Possible products of the antibody-catalyzed degradation Δ⁹-THC. (A) Primary metabolic products of Δ⁹-THC, 11-hydroxy-Δ⁹-tetrahydrocannabinol **1**, and 11-nor-9-carboxy-Δ⁹-tetrahydrocannabinol **2**; (B) postulated chemistry and degradation products of the antibody-catalyzed degradation Δ⁹-THC.

this precedent, two panels of Δ⁹-THC-binding antibodies[19] were examined in the present study, and all antibodies tested were found to catalyze the oxidative degradation of Δ⁹-THC. The major product from this transformation was identified using extensive spectroscopic analysis and an unexpected antibody-catalyzed reaction was revealed.

Results and Discussion

Considering that no reaction was observed in our previous study using tight binding nicotine antibodies ($K_{d,app} \leq 1\ \mu M$) and only weaker binding antibodies ($K_{d,app} = \mu M$ to mM) generated against a less congruent hapten were found to catalyze the oxidative degradation of the drug,[18] we were particularly interested in a range of Δ⁹-THC binding affinities in designing a screen for the antibody-catalyzed oxidative degradation of Δ⁹-THC. The structural nuances of the TCB and TCF haptens provided monoclonal antibodies with a wide affinity range for Δ⁹-THC and highlight two strategies employed in hapten design (Figure 1).[19] The TCB hapten is highly analogous to Δ⁹-THC with the linker positioned distal to any portion of the molecule anticipated to be essential for antibody recognition. In contrast, the TCF hapten has an aromatized C ring and additional amide bonds in the linker, sacrificing structural similarity in an attempt to elicit stronger immune responses.[12] The TCB hapten elicited tight binding antibodies with adequate serum titers, and several monoclonal antibodies from this panel possessed excellent affinity for Δ⁹-THC (TCB25G1, $K_d = 0.23\ \mu M$). As expected, higher serum titers were observed from TCF immunization; however, weaker Δ⁹-THC binding was observed for monoclonal antibodies from this panel ($K_d > 100\ \mu M$), presumably because the TCF hapten deviates too greatly from the structure of Δ⁹-THC. A screen using both panels was conducted by monitoring Δ⁹-THC concentration over time. Analogous to our previous studies, the weaker binding TCF panel (20 antibodies) provided more proficient catalysts, while the tighter binding TCB panel (5 antibodies) also catalyzed the degradation of Δ⁹-THC, albeit less proficiently.

The antibody-catalyzed oxidative degradation of Δ⁹-THC led to the formation of one major product and multiple minor products. Using the limited amount of major product obtained from the antibody screen, a molecular weight of 346 was measured by mass spectrometry corresponding to the addition of two oxygen atoms. The major urinary metabolites of Δ⁹-THC in humans are 11-hydroxy-Δ⁹-tetrahydrocannabinol **1** and

(18) Dickerson, T. J.; Yamamoto, N.; Janda, K. D. *Bioorg. Med. Chem.* **2004**, *12*, 4981−4987.
(19) Qi, L.; Yamamoto, N.; Meijler, M. M.; Altobell, L. J.; Koob, G. F.; Wirsching, P.; Janda, K. D. *J. Med. Chem.* **2005**, *48*, 7389−7399.

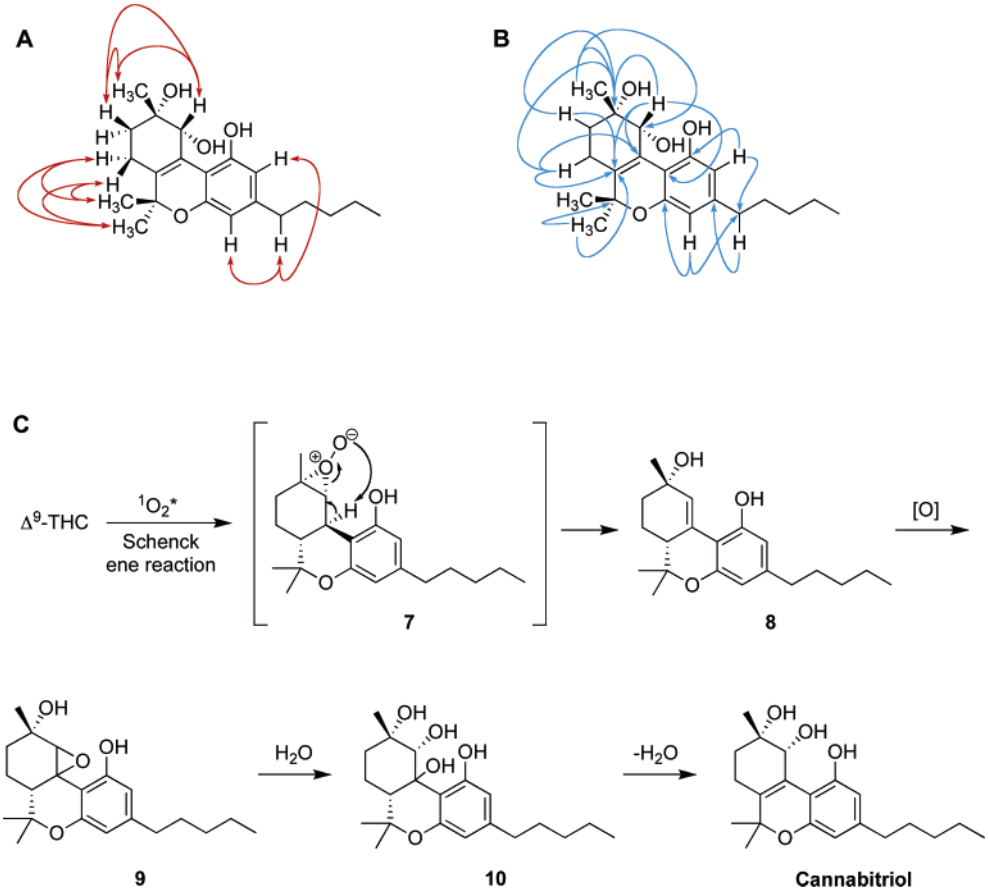

Figure 3. (A) Key ^{1}H-^{1}H ROESY correlations for cannabitriol; (B) key ^{1}H-^{13}C HMBC correlations for cannabitriol; (C) proposed antibody-catalyzed transformation of Δ^9-THC to cannabitriol.

11-nor-9-carboxy-Δ^9-tetrahydrocannabinol **2**;[20−22] however, neither of these compounds have a molecular weight corresponding to the unknown oxidation product. Given the potential for antibody-generated ROS, we also considered possible oxidation reactions, and in particular, the oxidation of the C9−C10 olefin. Ozonolysis of this olefin generates ketoaldehyde **3** that could subsequently undergo an intermolecular aldol reaction to yield *β*-hydroxyketone **4** or react with the neighboring phenol resulting in hemiacetal **5** (Figure 2). Another possibility is a [2+2] cycloaddition reaction with $^1O_2$* to yield the corresponding dioxetane **6**.

To identify the major product from the antibody-catalyzed degradation of Δ^9-THC, significant quantities were needed for spectroscopic analysis. Traditional synthetic organic chemistry techniques were employed by exposing Δ^9-THC to ozone and hydrogen peroxide in an attempt to mimic the chemistry occurring in the antibody-catalyzed reaction and also provide insight into oxidants involved. Ozonolysis of Δ^9-THC provided no identifiable products; however, trace amounts of the major product from the antibody-catalyzed degradation of Δ^9-THC were observed in the hydrogen peroxide reaction. In light of this limited success, we increased the scale of the antibody catalyzed reaction 100-fold and extended the time of the reaction. Throughout the course of the reaction additional aliquots of Δ^9-THC and riboflavin were added to maximize product yield.

With greater quantities of product now available, 1D and 2D NMR techniques were used to characterize the molecular composition of the antibody-catalyzed oxidation product. ^{1}H NMR revealed clear resonances for the hydrocarbon tail and the A-ring protons, and ^{13}C NMR verified that this portion of the molecule was intact. Three singlets corresponding to the C6 and C9 methyl groups remained along with multiplets for the C7 and C8 protons. Importantly, the C10 olefin proton and the protons on the tertiary carbons C6a and C10a were absent, and a new singlet at δ 4.2 emerged. In the ^{13}C NMR, two signals in the aromatic region of the spectrum at δ 122 and 136 in addition to resonances for the A ring were observed. The lack of ^{13}C NMR carbonyl signals eliminated the proposed ozonolysis product **3** and the subsequent aldol and hemiacetal products **4** and **5**. Resonances corresponding to dioxetane **6** were also inconsistent with the 1D and 2D NMR data, particularly the disconnect between the C7 and C8 protons and any other portion of the molecule in the ^{1}H-^{1}H COSY spectrum.

Deviating from our initial assumption of simple single-step oxidation reactions, we began to consider multistep pathways involving multiple oxidants and, after further examination of the NMR data, the oxidized Δ^9-THC analogue cannabitriol was considered as a possible product from the antibody-catalyzed degradation of Δ^9-THC (Figure 3). Cannibitriol is a native component of marijuana and was first isolated and characterized by von Spulak et al.[23] in 1968, with the stereochemistry later

(20) Huestis, M. A. *Handb. Exp. Pharmacol.* **2005**, *168*, 657−690.
(21) Grotenhermen, F. *Clin. Pharmacokinet.* **2003**, *42*, 327−360.
(22) McGilveray, I. J. *Pain Res. Manage.* **2005**, *10*, 15A-22A.
(23) Von Spulak, F.; Claussen, U.; Fehlhaber, H. W.; Korte, F. *Tetrahedron* **1968**, *24*, 5379−5383.

assigned.[24−26] The limited NMR data from these studies are consistent with the major product from the antibody-catalyzed oxidation of Δ⁹-THC. The singlet at δ 4.2 in the ^{1}H NMR spectrum corresponds to the C10 proton of cannabitriol, and the ^{13}C NMR signals at δ 122 and 136 correspond to the C6a−C10a double bond. The newly formed quaternary center at C9 and the C6a−C10a olefin of cannabitriol provide clarity for the disconnect between the C7 and C8 protons and any other portion of the molecule in the ^{1}H-^{1}H COSY spectrum. The additional hydroxyl groups of cannabitriol generate stereogenic centers at C9 and C10 and, through the use of a ^{1}H-^{1}H ROESY experiment, the stereochemistry was assigned as cis by through-space correlations between the C9-methyl protons and the C10 proton. Key correlations stemming from the oxidation of the C ring between the C6 methyl, C7, C8, and C10 protons and the C6a−C10a olefin were observed by ^{1}H-^{13}C HMBC, and the anticipated ^{1}H-^{13}C HMQC and ^{1}H-^{13}C HMBC correlations further supported the identity of the unknown as cannabitriol.

The identification of cannabitriol as the major product from the antibody-catalyzed oxidative degradation of Δ⁹-THC led us to explore the chemistry involved in this transformation (Figure 3C). A Schenck ene reaction between Δ⁹-THC and singlet oxygen was envisioned as the first step. Experimental and theoretical studies of the Schenk ene reaction mechanism are most consistent with perepoxide intermediate **7**, which differs distinctly from the typical pericyclic ene reaction mechanism using an olefin instead of $^1O_2$*.[27] Empirical data indicates that proton abstraction by the perepoxide nucleophilic oxygen occurs on the more highly substituted side of the olefin, which is the proton on C8 or C10a. However, selectivity for the proton on C10a is favored since the nascent olefin in **8** is in conjugation with the aromatic A ring, generating a more thermodynamically stable product. This initial reaction also sets the stereochemistry at C9 since perepoxide formation must occur on the less hindered side of the alkene, dictated by the stereochemistry of Δ⁹-THC, enabling the nucleophilic perepoxide oxygen to be proximal to the C10a proton. A second oxidant is then needed in an epoxidation reaction of the newly formed olefin at C10−C10a. Since there are few steric constraints, in bulk solution, the stereochemistry of epoxide **9** is dependent upon whether the subsequent epoxide ring opening reaction occurs at the thermodynamically favored C10a or the kinetically favored C10 position. Cis epoxidation, relative to the C9 hydroxyl, requires thermodynamic epoxide ring opening and subsequent elimination in order to obtain cannabitriol in the proper stereochemical configuration, whereas trans epoxidation requires kinetic epoxide ring opening and subsequent elimination. Unfortunately, additional clarity in the origin of the stereochemistry at C10 cannot be deduced from the elimination reaction of tetraol **10** since a putative tertiary carbocation at C10a favors an E1 mechanism with no syn or anti selectivity. In addition we cannot rule out the possibility that the antibody influences this reaction, causing one pathway to be favored.[28−30] Interestingly, the addition of catalase and superoxide dismutase (1 μM each) to the reaction mixture did not affect the rate of cannabitriol formation. This suggests that free hydrogen peroxide or superoxide radical are not involved in the oxidation of Δ⁹-THC, although the possibility that either oxidant is sequestered from the bulk water and utilized by the antibody cannot be discounted.[16,17] In total, the regio- and stereospecificity of the product suggests that the oxidation steps are catalyzed by the antibody, whereas, the epoxide ring opening and elimination reactions may occur in the bulk water.

Table 1. Kinetic Parameters for the Antibody-Catalyzed Conversion of Δ⁹-THC to Cannabitriol

antibody	k_{cat} (min^{-1})	k_{cat}/k_{uncat}	K_M (μM)	k_{cat}/K_M (min^{-1} μM^{-1})
TCF-26C12	0.999	1.97×10^4	275	3.63×10^{-3}
TCF-23C4	1.00	1.97×10^4	394	2.54×10^{-3}
TCF-25G5	1.00	1.97×10^4	595	1.68×10^{-3}
none	5.08×10^{-5}			

The kinetics of cannabitriol formation was measured for the three most proficient catalysts (TCF-26C12, TCF-23C4, and TCF-25G5). The high-energy states of photochemical reactions result in multiple products and, in order for the antibody-catalyzed transformation to dominate, a high concentration of antibody relative to the substrate is required for accurate measurements, invalidating the usual Michaelis−Menten approximation that free and total substrate concentrations are essentially equal. Therefore, in order to calculate the k_{cat} and K_M for the antibody-catalyzed formation of cannabitriol (eq 1) assuming saturating riboflavin conditions, the concentration of the antibody−substrate complex [AS] was explicitly determined (eq 2), where v_o is the initial reaction velocity, $[A] = [A]_t - [AS]$, and $[S] = [S]_f = [S]_t - [AS]$.[31]

$$v_o = k_{cat}[AS] \tag{1}$$

$$[AS] = \frac{([S]_t + [A]_t + K_M) - \sqrt{([S]_t + [A]_t + K_M)^2 - 4[S]_t[A]_t}}{2} \tag{2}$$

Each antibody measured catalyzed cannabitriol formation with approximately the same rate (Table 1). In examining the therapeutic potential of the antibody-catalyzed degradation of Δ⁹-THC, it is important to note that cannabitriol is not the only product from this reaction. Therefore, the k_{cat} for cannabitriol formation (1.0 min^{-1}) is a conservative estimate of the rate of drug degradation. The hydrophobic nature of Δ⁹-THC and accumulation in fatty tissue leads to an extended half-life ($t_{1/2}$) in vivo of more than 20 h.[22,32] Theoretical calculations using a 50 mg/kg dose of TCF-26C12 provide a blood concentration of approximately 5 μM, assuming that blood mass is equal to 7% of total body weight. An average dose of Δ⁹-THC (one 3.55% marijuana cigarette) leads to a peak blood concentration of approximately 0.5 μM; therefore, the antibody would be operating under substrate limiting conditions ($[S]_t \ll K_M$) and the rate equation can be simplified and a new rate constant

(24) ElSohly, M. A.; El-Feraly, F. S.; Turner, C. E. *Lloydia* **1977**, *40*, 275−280.
(25) ElSohly, M. A.; Boeren, E. G.; Turner, C. E. *Experientia* **1978**, *34*, 1127−1128.
(26) McPhail, A. T.; ElSohly, H. N.; Turner, C. E.; ElSohly, M. A. *J. Nat. Prod.* **1984**, *47*, 138−142.
(27) For a review of the Schenck ene reaction see: Prein, M.; Adam, W. *Angew. Chem., Int. Ed. Engl.* **1996**, *35*, 477−494.
(28) Janda, K. D.; Shevlin, C. G.; Lerner, R. A. *Science* **1993**, *259*, 490−493.
(29) Matsushita, H.; Yamamoto, N.; Meijler, M. M.; Wirsching, P.; Lerner, R. A.; Matsushita, M.; Janda, K. D. *Mol. Biosyst.* **2005**, *1*, 303−306.
(30) Sinha, S. C.; Keinan, E.; Reymond, J. L. *Proc. Natl. Acad. Sci. U.S.A.* **1993**, *90*, 11910−11913.
(31) Segel, I. H. *Enzyme Kinetics*; John Wiley & Sons: New York, 1975; pp 72−77.
(32) Gustafson, R. A.; Kim, I.; Stout, P. R.; Klette, K. L.; George, M. P.; Moolchan, E. T.; Levine, B.; Huestis, M. A. *J. Anal. Toxicol.* **2004**, *28*, 160−167.

derived, $k_{Ab} = 1.82 \times 10^{-2}$ min^{-1} (eq 3). Substituting k_{Ab} in the standard first-order half-life equation provides a $t_{1/2}$ of 38 min (eq 4). Thus, using the rate of cannabitriol formation as a conservative estimate, the normal metabolic half-life for Δ^9-THC can be reduced by more than 30-fold utilizing TCF-26C12.

$$v_o = \frac{k_{cat}[A]_t[S]_t}{K_M + [S]_t} \approx \frac{k_{cat}[A]_t[S]_t}{K_M} \approx k_{Ab}[S]_t,$$

$$\text{where } k_{Ab} = \frac{k_{cat}}{K_m}[A]_t \quad (3)$$

$$t_{1/2} = \frac{\ln 2}{k_{Ab}} \quad (4)$$

The antibody-catalyzed oxidative degradation of Δ^9-THC yields a structurally complex natural product that may have pharmacological activity. The physiological effects of Δ^9-THC and other cannabinoids stem from ligand binding to a family of cannabinoid receptors found primarily on central and peripheral neurons (CB_1) and immune cells (CB_2).[33] There is no reported pharmacological data for cannabitriol; therefore, the cytotoxicity of cannabitriol was measured in SH-SY5Y human neuroblastoma cells to examine CB_1-mediated neurotoxicity.[34] In this assay, Δ^9-THC and cannabitriol were found to be cytotoxic at similar concentrations ($EC_{50} = 5$ μM). However, the addition of two hydroxyl groups makes cannabitriol significantly more polar than Δ^9-THC by decreasing the ClogP nearly 3 orders of magnitude (Δ^9-THC ClogP = 7.2, cannabitriol ClogP = 4.4), thus reducing blood-brain barrier permeability.[35] Furthermore, the primary metabolic pathway of Δ^9-THC involves hydroxylation of the C ring, providing modification sites for glucoronidation. Although cannabitriol has cytotoxicity comparable to Δ^9-THC, the antibody-catalyzed degradation aids the natural metabolic pathways and is expected to facilitate elimination of the drug.

The conversion of Δ^9-THC to cannabitriol represents an antibody-catalyzed transformation that likely involves two different oxidants in a multistep chemical process. Catalysis is not programmed into the antibody by hapten design, unlike previous catalytic antibodies that employ transition-state analogues or reactive immunization, but rather is an inherent property of the antibody itself. This is significant considering the role $^1O_2$*-mediated oxidation may play in the respective therapeutic outcomes for the increasing number of monoclonal antibodies in the clinic and under development.[36] Furthermore, by specifically targeting the ability of an antibody to generate ROS from $^1O_2$*, we demonstrate the potential of the antibody-catalyzed oxidation of Δ^9-THC as a treatment for marijuana abuse.

Materials and Methods

General Procedures. All reagents were purchased from Sigma-Aldrich or Fisher and used as received. ^{1}H NMR and ^{13}C NMR spectra were recorded on a Bruker DRX-600 spectrometer equipped with a cryogenic probe at 600 and 150 MHz, respectively. Electrospray ionization (ESI) mass spectrometry experiments were performed on an Agilent ESI−TOF mass spectrometer. HPLC assays were performed on a Hitachi HPLC (model L-2130) equipped with a column oven (model L-2300) and UV detector (model L-2420) using Vydac RP-C_{18} columns.

HPLC Assay for the Conversion of Δ^9-THC to Cannabitriol. The rate constants for the antibody-catalyzed oxidative conversion of Δ^9-THC to cannabitriol were determined by the method of initial rates under pseudo-first-order conditions. Reactions were initiated by adding a solution of Δ^9-THC (50−400 μM) to phosphate buffer (PBS, pH 7.4) containing an antibody from the TCF or TCB panel (20 μM) and riboflavin (60 μM) to a final volume of 140 μL (5% DMSO). The reaction vessels were irradiated on a white light transilluminator (2.6 mW/cm^2) at 4 °C for various amounts of time, and aliquots (20 μL) were removed and injected onto the previously described HPLC system, equipped with a guard column (isocratic mobile phase: 51% A (water with 0.1% TFA) and 49% B (acetonitrile with 0.09% TFA), solvent flow rate of 1 mL min^{-1}; UV detection at 240 nm; 50 °C). Each assay was performed in duplicate, and data were quantified by interpolation of peak areas relative to a standard curve.

Synthesis of Cannabitriol via the Antibody Catalyzed Oxidation of Δ^9-THC. A solution of Δ^9-THC (5 mM), antibodies from the TCF and TCB panels (~14 μM), and riboflavin (90 μM) in phosphate buffer (PBS, pH 7.4) (5% DMSO) was irradiated on a white light transilluminator (2.6 mW/cm^2) at 4 °C. The reaction was monitored by the previously described HPLC assay, and additional aliquots of Δ^9-THC and riboflavin were added twice daily for a period of 4 days. The reaction mixture was extracted with diethyl ether and the combined organic layers were concentrated. The crude mixture was isolated by preparative HPLC (53% A (water with 0.1% TFA) and 47% B (acetonitrile with 0.09% TFA), solvent flow rate of 10 mL min^{-1}; UV detection at 240 nm; retention time of cannabitriol, 35.3 min). Fractions were collected at 0.5 min intervals in test tubes containing 1 mL of diethyl ether and 100 μL of saturated $NaHCO_3$. The fractions containing cannabitriol were combined, separated, and further extracted with diethyl ether (2×). The organic layers were combined and dried over anhydrous Na_2SO_4, filtered, and concentrated in vacuo. This procedure was performed twice for a total of 360 μg (the amount of cannabitriol was determined by NMR using 2,5-dimethylfuran as an internal standard).[37] ^{1}H NMR ($CDCl_3$) δ: 0.88 (t, J = 6.4 Hz, 3 H, H_3-5′), 1.24 (s, 3 H, CH_3-6), 1.26−1.36 (m, 4 H, H_2-4′, 3′H_2), 1.40 (s, 3 H, CH_3-9), 1.46 (s, 3 H, CH_3-6), 1.58 (m, 2 H, H_2-2′), 1.77−1.80 (m, 2 H, H_2-8), 2.15 (dt, J = 3.9, 19.0 Hz, 1 H, *H*H′-7), 2.39−2.46 (m, 1 H, H*H*′-7), 2.47 (t, J = 7.8 Hz, 2 H, H_2-1′), 4.20 (s, 1 H, H-10), 6.30 (s, 1 H, H-1 or H-4), 6.35 (s, 1 H, H-1 or H-4). ^{13}C NMR ($CDCl_3$) δ: 14.0 (C5′), 22.5 (C7), 22.6 (C4′), 23.5 (C6-*C*H$_3$), 25.1 (C9-*C*H$_3$), 25.3 (C6-*C*H$_3$), 29.1 (C8), 30.5 (C2′), 31.4 (C3′), 35.6 (C1′), 70.4 (C9), 72.4 (C10), 76.5 (C6), 108.9 (C1a), 109.2 (C2 or C4), 110.9 (C2 or C4), 122.1 (C10a), 136.1 (C6a), 144.8 (C3), 152.3 (C1 or C4a), 153.7 (C1 or C4a). All structural assignments were in agreement with the ^{1}H-^{1}H COSY, ^{1}H-^{1}H NOESY, ^{1}H-^{1}H ROESY, ^{1}H-^{13}C HMQC, ^{1}H-^{13}C HMBC, and ^{13}C APT data. MS (electrospray): m/z 347 $[M+1]^+$. HRMS (electrospray): m/z calcd for $C_{21}H_{31}O_4$, 347.2217 $[M+1]^+$; found, 347.2205

Acknowledgment. This work was supported by The Skaggs Institute for Chemical Biology, the National Institute on Drug Abuse (Grant DA 15700 to K.D.J.), and NIH Kirchstein postdoctoral fellowships (DA 18507 to A.P.B. and AI 62014 to L.M.E.).

Supporting Information Available: Synthesis of Δ^9-THC, full HMBC correlations, and NMR spectra. This material is available free of charge via the Internet at http://pubs.acs.org.

JA070022M

(33) Pertwee, R. G. *Handb. Exp. Pharmacol.* **2005**, *168*, 1−51.
(34) Klegeris, A.; Bissonnette, C. J.; McGeer, P. L. *Br. J. Pharmacol.* **2003**, *139*, 775−786.
(35) Ecker, G. F.; Noe, C. R. *Curr. Med. Chem* **2004**, *11*, 1617−1628.
(36) *Adv. Drug Delivery Rev.* **2006**, *58*, 631−766.
(37) Gerritz, S. W.; Sefler, A. M. *J. Comb. Chem* **2000**, *2*, 39−41.